Confidence Intervals of Modal Parameters during Progressive Damage Test

Michael Döhler, Falk Hille, Xuan-Binh Lam, Laurent Mevel and Werner Rücker

Abstract In Operational Modal Analysis, the modal parameters (natural frequencies, damping ratios and mode shapes) obtained from Stochastic Subspace Identification (SSI) of a structure, are afflicted with statistical uncertainty. For evaluating the quality of the obtained results it is essential to know the respective confidence intervals of these figures. In this paper we present algorithms that automatically compute the confidence intervals of modal parameters obtained from covariance- and data-driven SSI of a structure based on vibration measurements. They are applied to the monitoring of the modal parameters of a prestressed concrete highway bridge during a progressive damage test that was accomplished within the European research project IRIS. Results of the covariance- and data-driven SSI are compared.

1 Introduction

Subspace-based linear system identification methods have been proven efficient for the identification of the eigenstructure of a linear multivariable system in many applications. In this paper, the main motivation is output-only structural identification in vibration mechanics, of a structure subject to ambient unmeasured vibrations. The obtained modal parameters (natural frequencies, damping ratios and mode shapes) are afflicted with a statistical uncertainty, e.g. due to measurement noise, unstationarities in the excitation, or measurement data that may not be long enough to assume convergence of the identification method. For evaluating the quality of the identified modal parameters it is essential to know the respective confidence intervals of these

Michael Döhler, Xuan-Binh Lam, Laurent Mevel
INRIA, Centre Rennes - Bretagne Atlantique, Campus de Beaulieu, F-35042 Rennes, France,
e-mail: michael.dohler@inria.fr, xuan.lam@inria.fr, laurent.mevel@inria.fr

Falk Hille, Werner Rücker
BAM Federal Institute for Material Research and Testing, Division Buildings and Structures, D-12200 Berlin, Germany, e-mail: falk.hille@bam.de, werner.ruecker@bam.de

figures, especially when evaluating changes in a system (e.g. due to damage) where identified modal parameters are compared.

The problem consists in quantifying the uncertainty related to the identified modal parameters of a structure subject to ambient unmeasured vibrations. In [9], an algorithm was derived to automatically compute confidence intervals in covariance driven SSI, based on [8]. In [4] and [5], some propositions were made that improve this algorithm in efficiency and generality. Using covariance driven SSI and data driven SSI with the Unweighted Principal Component Algorithm (UPC), the resulting algorithm is applied in this paper on the S101 Bridge in Austria to compute confidence intervals, together with an automated monitoring procedure, during the progressive damage test of the bridge.

2 Stochastic Subspace Identification

2.1 State Space Model

The mechanical system is supposed to be a stationary linear dynamical system

$$\begin{cases} M\ddot{\mathscr{Z}}(t)+C\dot{\mathscr{Z}}(t)+K\mathscr{Z}(t) = v(t) \\ Y(t) = L\mathscr{Z}(t) \end{cases},$$

with

- $\mathscr{Z}$: displacements of the degrees of freedom,
- M, C, K: mass, damping, stiffness matrices,
- t: continuous time,
- v: excitation (Gaussien, zero-mean, white),
- L: observation matrix giving the observation Y.

The modal characteristics

- μ vibration modes or eigenfrequencies
- ψ_μ modal shapes or eigenvectors

are solutions of the following equation:

$$(M\mu^2+C\mu+K)\Psi_\mu = 0 \ , \ \psi_\mu = L\Psi_\mu.$$

We switch to the state space model in discrete time by sampling at the rate $1/\delta$ with

$$X_k = \begin{bmatrix} \mathscr{Z}(k\delta) \\ \dot{\mathscr{Z}}(k\delta) \end{bmatrix} \ , \ Y_k = Y(k\delta)$$

and get

$$\begin{cases} X_{k+1} = FX_k+V_k \\ Y_k = HX_k \end{cases}. \tag{1}$$

The modal characteristics (μ, ψ_μ) are given by the eigenstructure (λ, Φ_λ) of F:

$$e^{\delta\mu} = \lambda$$
$$\psi_\mu = \phi_\lambda \stackrel{\Delta}{=} H\Phi_\lambda$$

In the sequel the dimension of the observed output Y is much smaller than the dimension of the state X.

2.2 Identification Procedure

Knowing the output data Y_k at the time instants $k = 1,\ldots,N$, the eigenstructure (λ, ϕ_λ) of system (1) is identified with Stochastic Subspace Identification algorithms. In this work, the covariance driven approach [2, 7] and data driven approach with the Unweighted Principal Component algorithm [6, 7] are used.

For both approaches the parameters p and q are chosen as variables with $(p+1)r \geq qr \geq n$ with the desired model order n. Usually, $p+1 = q$ is set [1]. The data matrices

$$\mathscr{Y}_{p+1}^{+} \stackrel{\text{def}}{=} \begin{pmatrix} Y_{q+1} & Y_{q+2} & \vdots & Y_{N-p} \\ Y_{q+2} & Y_{q+3} & \vdots & Y_{N-p+1} \\ \vdots & \vdots & \vdots & \vdots \\ Y_{q+p+1} & Y_{q+p+2} & \vdots & Y_N \end{pmatrix}, \quad \text{and} \quad \mathscr{Y}_{q}^{-} \stackrel{\text{def}}{=} \begin{pmatrix} Y_q & Y_{q+1} & \vdots & Y_{N-p-1} \\ Y_{q-1} & Y_q & \vdots & Y_{N-p-2} \\ \vdots & \vdots & \vdots & \vdots \\ Y_1 & Y_2 & \vdots & Y_{N-p-q} \end{pmatrix} \quad (2)$$

are built, and, according to the method, a subspace matrix as follows:

- For the **covariance driven** approach, the subspace matrix

  $$\mathscr{H}_{p+1,q}^{\text{cov}} \stackrel{\text{def}}{=} \mathscr{Y}_{p+1}^{+}\mathscr{Y}_{q}^{-T}$$

  is built. It has the factorization property

  $$\mathscr{H}_{p+1,q}^{\text{cov}} = \mathscr{O}_{p+1}\, F\, \mathscr{C}_q$$

  with the matrix of observability

  $$\mathscr{O}_{p+1} = \begin{pmatrix} H \\ HF \\ \vdots \\ HF^p \end{pmatrix}$$

  and the matrix of controllability $\mathscr{C}_q$.

- For the Unweighted Principle Component algorithm of the **data driven** approach, the matrix

$$\mathscr{H}_{p+1,q}^{\text{data}} \stackrel{\text{def}}{=} \mathscr{Y}_{p+1}^{+} \mathscr{Y}_{q}^{-T} \left(\mathscr{Y}_{q}^{-} \mathscr{Y}_{q}^{-T} \right)^{-1} \mathscr{Y}_{q}^{-}$$

is defined. It enjoys the factorization property

$$\mathscr{H}_{p+1,q}^{\text{data}} = \mathscr{O}_{p+1} \mathscr{X}_{q} \tag{3}$$

into matrix of observability and Kalman filter state sequence. As $\mathscr{H}_{p+1,q}^{\text{data}}$ is usually a very big matrix and difficult to handle, a thin RQ decomposition of the data matrices is done at first:

$$\begin{pmatrix} \mathscr{Y}_{q}^{-} \\ \mathscr{Y}_{p+1}^{+} \end{pmatrix} = RQ = \begin{pmatrix} R_{11} & 0 \\ R_{21} & R_{22} \end{pmatrix} \begin{pmatrix} Q_1 \\ Q_2 \end{pmatrix}.$$

Then, $\mathscr{H}_{p+1,q}^{\text{data}} = R_{21} Q_1$ follows and the subspace matrix is defined as

$$\mathscr{H}_{p+1,q}^{\text{data,R}} = R_{21},$$

which enjoys also factorization property (3), but with a different matrix on the right side. See also [6] for further details.

In what follows, the superscripts of the subspace matrix $\mathscr{H}_{p+1,q}$ are skipped, as the identification procedure is the same for the covariance and data driven approach. Now we want to obtain the eigenstructure of the system (1) from a given matrix $\mathscr{H}_{p+1,q}$. The observability matrix $\mathscr{O}_{p+1}$ is obtained from a thin SVD of the matrix $\mathscr{H}_{p+1,q}$ and its truncation at the desired model order n:

$$\begin{aligned} \mathscr{H}_{p+1,q} &= U \, \Delta \, V^T \\ &= \begin{pmatrix} U_1 & U_0 \end{pmatrix} \begin{pmatrix} \Delta_1 & 0 \\ 0 & \Delta_0 \end{pmatrix} V^T, \\ \mathscr{O}_{p+1} &= U_1 \, \Delta_1^{1/2}. \end{aligned} \tag{4}$$

The observation matrix H is then found in the first block-row of the observability matrix $\mathscr{O}_{p+1}$. The state-transition matrix F is obtained from the shift invariance property of $\mathscr{O}_{p+1}$, namely

$$\mathscr{O}_{p}^{\uparrow}(H,F) = \mathscr{O}_{p}(H,F) \, F, \quad \text{where } \mathscr{O}_{p}^{\uparrow}(H,F) \stackrel{\text{def}}{=} \begin{pmatrix} HF \\ HF^2 \\ \vdots \\ HF^p \end{pmatrix}. \tag{5}$$

Of course, for recovering F, it is needed to assume that $\operatorname{rank}(\mathscr{O}_p) = \dim F$, and thus that the number $p+1$ of block-rows in $\mathscr{H}_{p+1,q}$ is large enough. The eigenstruc-

ture (λ, ϕ_λ) results from

$$\det(F - \lambda\, I) = 0,\;\; F\;\varphi_\lambda = \lambda\;\varphi_\lambda,\;\; \phi_\lambda = H\varphi_\lambda, \tag{6}$$

where λ ranges over the set of eigenvalues of F.

In practice, the truncation order of the SVD is increased from 1 to the maximal system order in Equation (4) to get a stabilization diagram of the obtained modes vs model order. This gives results for successive different but redundant models and modes that are common to many successive models can be distinguished from the spurious modes.

There are many papers on the used identification techniques. A complete description can be found in [2, 6, 7, 3], and the related references. A proof of non-stationary consistency of these subspace methods can be found in [3].

3 Confidence Interval Computation

The statistical uncertainty of the obtained modal parameters is necessary to assess the confidence one can have in these values, e.g. when comparing the modal parameters of different states of a structure. Modal parameters with little confidence (and hence large confidence intervals) are little useful for comparing structural states.

The uncertainties of the modal parameters at a chosen system order can be computed from the uncertainty of the subspace matrix by doing a sensitivity analysis, and the covariance of the subspace matrix $\Sigma_{\mathscr{H}}$ can be evaluated by cutting the sensor data into blocks on which instances of the subspace matrix are computed. It holds

$$\Delta f_j = \mathscr{J}_{f_j}\,\Delta(\mathrm{vec}\,\mathscr{H}),\quad \Delta d_j = \mathscr{J}_{d_j}\,\Delta(\mathrm{vec}\,\mathscr{H}),\quad \Delta\varphi_j = \mathscr{J}_{\varphi_j}\,\Delta(\mathrm{vec}\,\mathscr{H}),$$

with the frequencies f_j, damping ratios d_j and mode shapes φ_j, and their sensitivities $\mathscr{J}$ with respect to $\mathrm{vec}\,\mathscr{H}$. It follows

$$\mathrm{cov} f_j = \mathscr{J}_{f_j}\Sigma_{\mathscr{H}}\,\mathscr{J}_{f_j}^T,\quad \mathrm{cov} d_j = \mathscr{J}_{d_j}\Sigma_{\mathscr{H}}\,\mathscr{J}_{d_j}^T,\quad \mathrm{cov}\varphi_j = \mathscr{J}_{\varphi_j}\Sigma_{\mathscr{H}}\,\mathscr{J}_{\varphi_j}^T.$$

This offers a possibility to compute confidence intervals on the modal parameters at a certain system order without repeating the system identification. In [9] this algorithm was described in detail for the covariance-driven SSI.

In this paper, three extensions of the confidence interval computation of [9] are used:

- As the mode shapes are defined up to a complex constant, the confidence interval computation on them requires an additional constraint. In [9], the confidence intervals are computed with respect to one point of the mode shape that is normalized to value one, which results in a confidence interval of size zero of this point. In [4], the confidence intervals of the mode shapes are computed with respect to the maximal amplitude of deflection, which is applied in this paper.

- The sensitivity computation of $\mathscr{J}_{f_j}$, $\mathscr{J}_{d_j}$ and $\mathscr{J}_{\varphi_j}$ depends on the sensitivities of the singular vectors of $\mathscr{H}$. In [5], an efficient computation was derived, which is applied here.
- Also in [5], the computation of $\Sigma_{\mathscr{H}}$ was extended to the data driven UPC subspace matrix.

4 Modal Analysis of S101 Bridge during Progressive Damage Test

Within the European research project "Integrated European Industrial Risk Reduction System (IRIS)" the prestressed concrete bridge S01 was artificially damaged [10]. The damaging processes were accompanied with a permanent measurement of the static and dynamic behavior of the structure. With that action a complete record of monitoring data during a defined loss of structural integrity on a typical bridge structure could be provided to test and evaluate SHM methods and applications.

4.1 The S101 Bridge

The S101 was a prestressed concrete bridge from the early 1960th spanning over the 4-lane highway A1 in Austria. The structural system was a three-field frame with a 32 m wide mean field and two 12 m wide side fields. The superstructures cross section was designed as a 7.2 m wide post-tensioned double T-beam with varying heights (Figure 1).

During recurring technical inspections of the bridge several deficiencies as cracks and spellings have been found. Since the crack pattern correlated with the geometric properties of the prestressing a significant deficit of structural reliability was assumed. Because of the subsequent determined limited load bearing capacity it was decided to replace the structure.

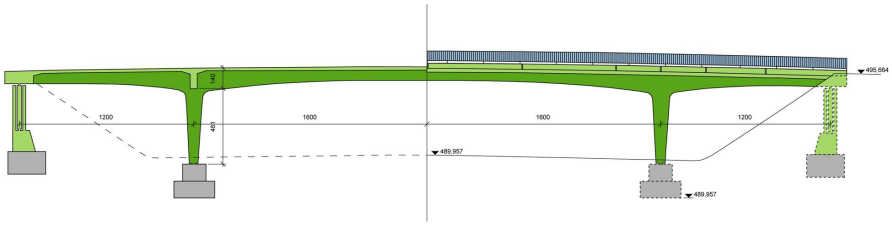

Fig. 1 System drawing of bridge S101 [10].

4.2 Measurement Description

The measurement campaign was carried out by the Austrian company VCE and the University of Tokyo [10]. For vibration measurement a BRIMOS measurement system containing a permanent sensor grid was used. The grid consisted out of 15 sensor locations on the bridge deck, see Figure 2, in each location three sensors for measurement in the bridge decks vertical, longitudinal and transversal direction. All in all, for vibration measurement 45 acceleration sensors were applied. Additionally, for verification of the static response of the structure to the damaging, the vertical displacement of the bridge deck was measured in three characteristic locations.

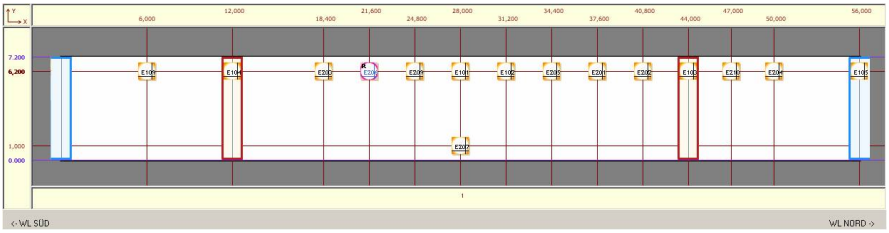

Fig. 2 Bridge deck with sensor grid for vibration measurement, on each location acceleration was measured in three directions [10].

The measurement took place with a sampling frequency of 500 Hz. All values were recorded permanently and stored in files with 165000 data points each. During the three days measurement campaign 714 data files each containing 48 channels were produced.

The damage test took place between the 10 and 13 December 2008. Because of the time in year and because of clouds the variation of the bridge temperature over the whole period of the test was minimal. During the test the highway beneath the bridge was open in one direction. Therefore dynamic excitations from moving trucks can be found in the signals. The second direction was closed for traffic because of construction work which in addition took place near the bridge. Perturbation of the measurement signals by the undergoing road construction work cannot be ruled out.

4.3 Damage Description

Prior to the demolition of the bridge a destructive damage test for measuring and investigating the structural behavior during damaging processes could be arranged and carried out. The campaign was planed and organized by VCE [10].

Two major damage scenarios were artificially induced. First, a significant damage on one of the four columns was reproduced by cutting through the column on its

Fig. 3 Destructive damaging; a) cutting through one of the columns, b) and c) successive intersecting of prestressing tendons [10].

A	First cut through column	G	Uplifting column
B	Second cut through column	H	Exposing cables and cut through first cable
C	Lowering column (first step)	I	Cut through second cable
D	Lowering column (second step)	J	Cut through third cable
E	Lowering column (third step)	K	Cut through fourth cable
F	Inserting steel plates		

Table 1 Damage scenarios during progressive damage test of S101 bridge.

lower end. With this action a change in the global structural system was to be implemented. After a second cut a 5 cm slice of the column was removed and the column was lowered for altogether 3 cm until the elastic ductility of the bridge structure was depleted (Figure 3).

Afterwards the column was uplifted again to its original position and secured there by steel plates. In a second damage scenario prestressing tendons of one of the beams were to be cut successively (Figure 3). Since the loss of prestressing by deterioration processes is a typical risk for existing RC bridges it was of specific interest to examine the sensitivity of damage identification routines to that kind of structural degradation. All in all three and a quarter of a wire bundle were cut through. Between each intersection pauses of several hours were kept to let the structural system change into a new state of equilibrium. For safety reasons the damaging process was stopped after 3.25 tendons were intersected. An overview of all introduced damages is given in Table 1.

4.4 System Identification Results before Destruction

In this paper, primary interest is in the identification of the first five modes in the frequency range [0–18 Hz]. For this, the data was downsampled from sampling rate 500 Hz by factor 8 and after a first examination only the sensors in vertical direction were chosen, as in this frequency range only vertical bending and torsional modes were present. System identification and confidence interval computation was done with the covariance and data driven SSI methods from Section 2.2 with parameters

$p+1=q=11$ at system orders $n=1,\ldots,70$. Confidence bounds were obtained by cutting the data into 100 blocks.

In Figure 4, the stabilization diagrams of the natural frequencies from both SSI methods are presented, where the confidence interval of each frequency is plotted as a horizontal bar. The obtained confidence bounds on the frequencies were used to clean the diagrams: Modes with frequencies having big confidence bounds are likely to be spurious and are erased. In this case, all modes with confidence bounds bigger than 2% of the frequency value were deleted.

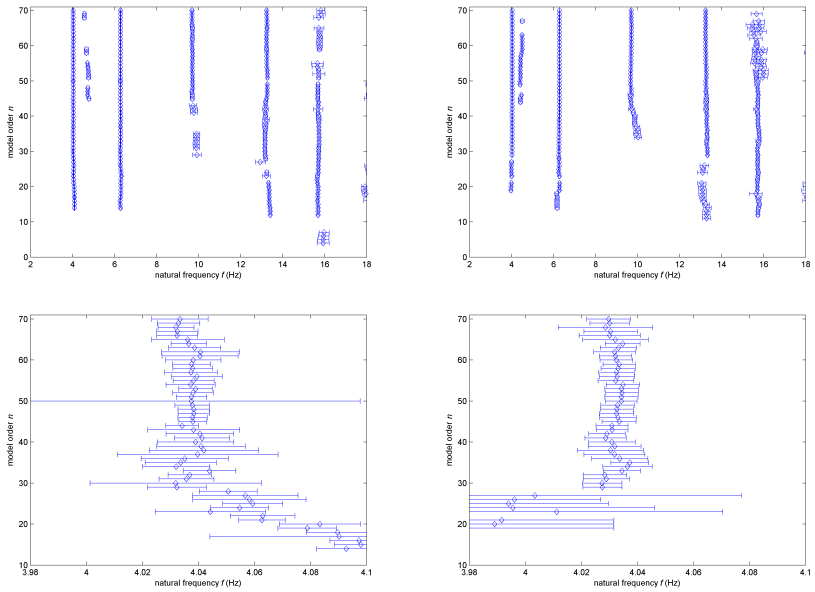

Fig. 4 Stabilization diagrams with covariance driven SSI (left) and data driven SSI (right) containing confidence intervals on the frequencies (top: full diagrams, bottom: zoom on first mode).

From the stabilization diagrams, the modes of the system are chosen. In Table 2, an overview of the obtained modal parameters and their confidence bounds at model order 40 is given. Note that all confidence bounds are relative values in percent, i.e. the standard deviation of a value divided by the value and multiplied by 100. For the mode shapes, only the relative confidence bound is displayed for the mode shape element of maximal amplitude.

Finally, the obtained mode shapes at the 14 sensors of one side of the bridge deck are displayed with their confidence bounds in Figure 5. From the 15th sensor on the other side of the bridge deck (see also Figure 2), information about the kind of the mode is obtained. So, modes 1, 3 and 5 are vertical bending modes and modes 2 and 4 are torsional modes.

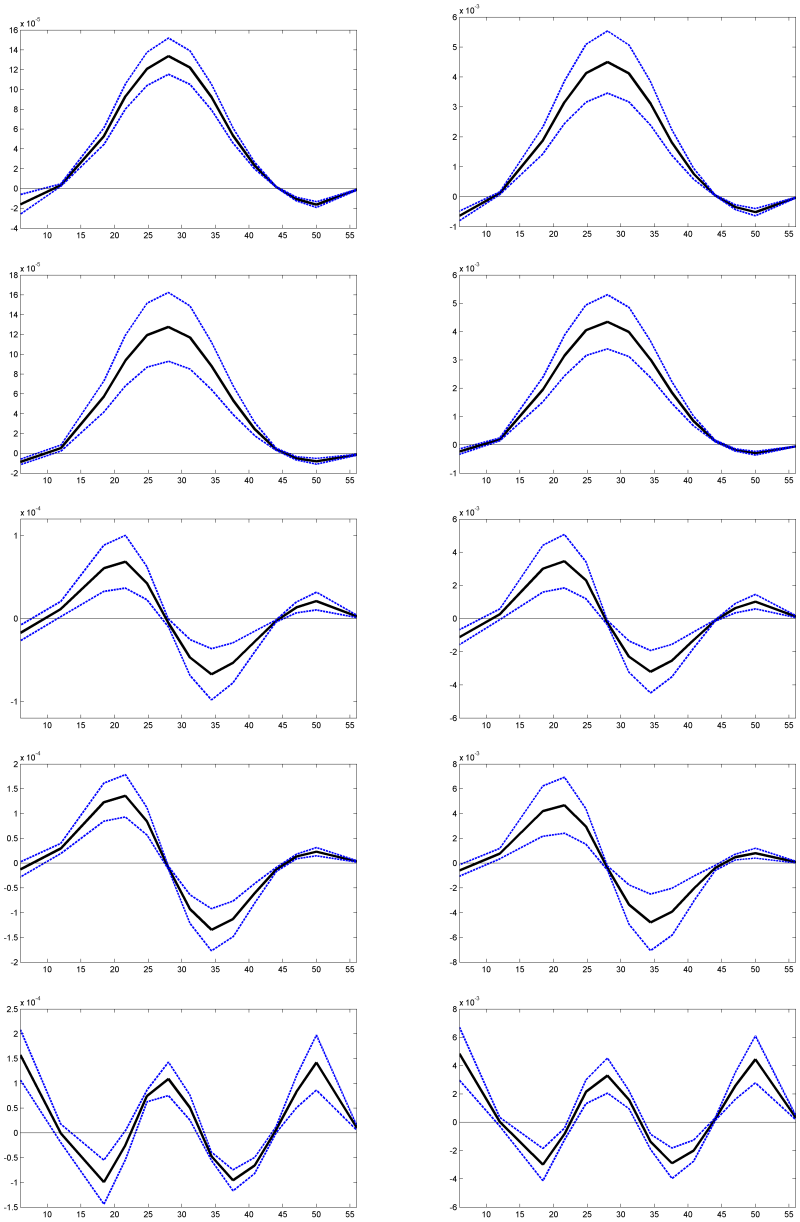

Fig. 5 First five mode shapes with their confidence bounds from covariance driven SSI (left) and data driven SSI (right).

	Covariance driven SSI					Data driven SSI (UPC)				
mode	f (in Hz)	$\tilde{\sigma}_f$	d (in %)	$\tilde{\sigma}_d$	$\tilde{\sigma}_{\varphi_{\max}}$	f (in Hz)	$\tilde{\sigma}_f$	d (in %)	$\tilde{\sigma}_d$	$\tilde{\sigma}_{\varphi_{\max}}$
1	4.039	0.34	1.1	23	13	4.031	0.21	1.3	22	22
2	6.292	0.19	0.6	52	27	6.282	0.11	0.7	19	22
3	9.730	3.42	3.0	92	47	9.872	1.17	2.1	32	46
4	13.19	0.67	1.3	73	31	13.31	0.38	1.4	22	48
5	15.72	0.70	1.8	20	32	15.73	0.39	1.8	19	39

Table 2 Overview of the estimated first 5 modes of S101 Bridge with natural frequencies f, their relative confidence bounds $\tilde{\sigma}_f = \sigma_f / f \cdot 100$, the damping ratios d, their relative confidence bounds $\tilde{\sigma}_d = \sigma_d / d \cdot 100$ and the relative confidence bounds of the mode shape element of maximal amplitude $\tilde{\sigma}_{\varphi_{\max}} = \sigma_{\varphi_{\max}} / \varphi_{\max} \cdot 100$.

To summarize the system identification results from covariance and data driven SSI, it can be said that both approaches give practically identical estimates in this test case when taking the obtained confidence bounds into account. However, the data driven approach seems to yield frequency and damping estimates that have lower confidence bounds than the covariance driven approach. Confidence bounds for the mode shape estimates are comparable for both approaches.

Confidence bounds are low on modes that seem to have stabilized in the stabilization diagram (e.g. on modes 1 and 2 at model order 40), while they are high on modes that have not stabilized yet (e.g. mode 3 at model order 40). Confidence bounds on frequency estimates are very low (lower than 1% on stabilized modes), while they are much higher on damping and mode shape estimates.

4.5 Monitoring during Progressive Damage Test

During the progressive damage test of the S101 Bridge, more than 700 datasets were available. Some of them contained erroneous data due to destruction work on the bridge or other influences that were deleted. On the left 680 datasets, an automated monitoring procedure was applied, that did the system identification and confidence interval computation automatically for each dataset. This means, that for each dataset a stabilization diagram was built with the SSI algorithms, containing model orders from 10 to 70. Then, the modes were chosen automatically using stabilization criteria such as thresholds for the damping estimates and confidence interval bounds, small frequency deviation between successive model orders, a minimum number of appearances of a frequency in the diagram and the MAC value between successive model orders.

The results of the frequency monitoring of all datasets are displayed in Figure 6 and the respective damage scenarios are explained in Table 1. Especially the frequency drop can be clearly seen when one column of the bridge was lowered before it was lifted up again (between A and G). This affected mainly the second, third and fourth mode, while the frequency changes in the first mode were less important. Es-

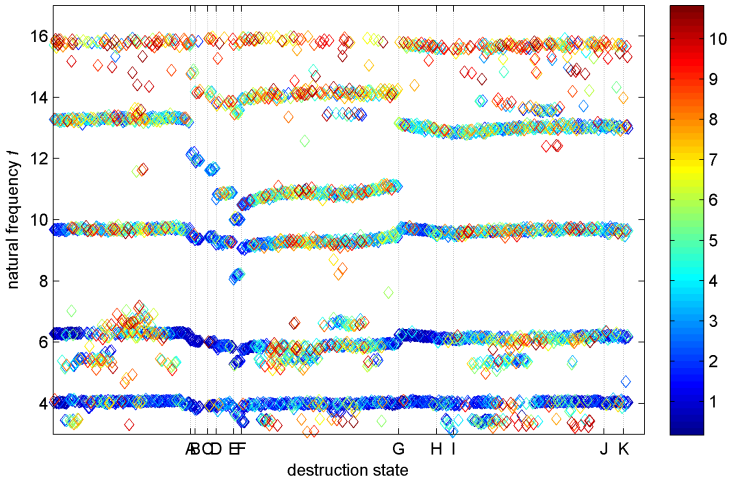

(a) covariance driven SSI

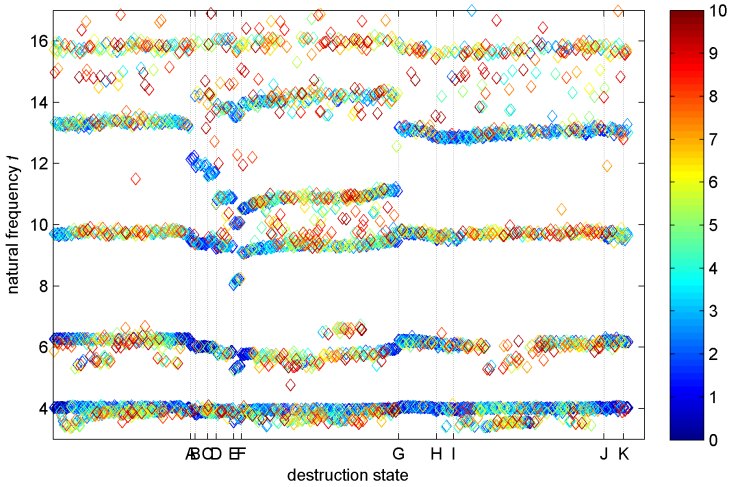

(b) data driven SSI (UPC)

Fig. 6 Natural frequencies with confidence bounds during progressive damage test of S101 Bridge (damage incidents from Table 1). The color bar indicates the confidence bound in percent of the obtained frequency.

pecially the change in the fourth mode is remarkable, as it split in two modes during the lowering of the column, with one lower and one higher frequency than before. The frequency changes in the fifth mode cannot be evaluated, as its uncertainty is very high compared to the other modes.

Also, the change in the frequencies when cutting the tendons (between G and K) is not significant. Only after the uplifting of the column and before cutting the first tendon (between G and H), some of the frequencies are dropping, probably due to the settling of the structural system after the uplifting. However, no significant change in the frequencies can be observed afterwards.

5 Conclusion

In this paper, confidence intervals on modal parameters during a progressive damage test were successfully computed with an improved algorithm. Using an automated monitoring procedure, the modal parameters of the S101 Bridge during this damage test were obtained completely automatically together with their confidence bounds. The artificially introduced damage scenarios "lowering of a column" could be clearly linked to changes in the natural frequencies, while "cutting the tendons" did not have a significant influence on the frequencies. It was shown that the confidence bounds on the modal parameters are essential when evaluating the changes in the modal parameters of the structure due to the introduced damages.

System identification results obtained by covariance and data driven SSI are very similar, with slightly lower confidence bounds for results obtained from data driven SSI with UPC.

Acknowledgments

This work was partially supported by the European project FP7-NMP CP-IP 213968-2 IRIS. We also thank VCE for providing the data from S101 Bridge.

References

1. Basseville, M., Benveniste, A., Goursat, M., Hermans, L., Mevel, L., van der Auweraer, H.: Output-only subspace-based structural identification: from theory to industrial testing practice. Journal of Dynamic Systems, Measurement, and Control **123**(4), 668–676 (2001)
2. Benveniste, A., Fuchs, J.J.: Single sample modal identification of a non-stationary stochastic process. IEEE Transactions on Automatic Control **AC-30**(1), 66–74 (1985)
3. Benveniste, A., Mevel, L.: Non-stationary consistency of subspace methods. IEEE Transactions on Automatic Control **AC-52**(6), 974–984 (2007)
4. Döhler, M., Lam, X.B., Mevel, L.: Confidence intervals on modal parameters in stochastic subspace identification. In: Proceedings of the 34th IABSE Symposium. Venice, Italy (2010)

5. Döhler, M., Mevel, L.: Robust subspace based fault detection. Tech. Rep. 7427, INRIA (2010). Submitted to 18th IFAC World Congress
6. van Overschee, P., De Moor, B.: Subspace Identification for Linear Systems: Theory, Implementation, Applications. Kluwer (1996)
7. Peeters, B., De Roeck, G.: Reference-based stochastic subspace identification for output-only modal analysis. Mechanical Systems and Signal Processing **13**(6), 855–878 (1999)
8. Pintelon, R., Guillaume, P., Schoukens, J.: Uncertainty calculation in (operational) modal analysis. Mechanical Systems and Signal Processing **21**(6) (2007)
9. Reynders, E., Pintelon, R., De Roeck, G.: Uncertainty bounds on modal parameters obtained from stochastic subspace identification. Mechanical Systems and Signal Processing **22**(4), 948–969 (2008)
10. VCE: Progressive damage test S101 Flyover Reibersdorf / draft. Tech. Rep. 08/2308, VCE (2009)